AD_____

Award Number: W81XWH-10-1-0087

TITLE: Sympathetic Nerves in Breast Cancer: Angiogenesis and Antiangiogenic Therapy

PRINCIPAL INVESTIGATOR: Dr. Kelley Madden

CONTRACTING ORGANIZATION: University of Rochester
Rochester, NY 14611

REPORT DATE: February 2011

TYPE OF REPORT: Annual

PREPARED FOR: U.S. Army Medical Research and Materiel Command
Fort Detrick, Maryland 21702-5012

REPORT DOCUMENTATION PAGE

Form Approved
OMB No. 0704-0188

1. REPORT DATE *(DD-MM-YYYY)*	**2. REPORT TYPE**	**3. DATES COVERED** *(From - To)*
01-02-2011	Annual	1 FEB 2010 - 31 JAN 2011

4. TITLE AND SUBTITLE
Sympathetic Nerves in Breast Cancer: Angiogenesis and Antiangiogenic Therapy

5a. CONTRACT NUMBER

5b. GRANT NUMBER
W81XWH-10-1-0087

5c. PROGRAM ELEMENT NUMBER

6. AUTHOR(S)
Dr. Kelley Madden

E-Mail: kelley_madden@urmc.rochester.edu

5d. PROJECT NUMBER

5e. TASK NUMBER

5f. WORK UNIT NUMBER

7. PERFORMING ORGANIZATION NAME(S) AND ADDRESS(ES)
University of Rochester
Rochester, NY 14611

8. PERFORMING ORGANIZATION REPORT NUMBER

9. SPONSORING / MONITORING AGENCY NAME(S) AND ADDRESS(ES)
U.S. Army Medical Research and Materiel Command
Fort Detrick, Maryland 21702-5012

10. SPONSOR/MONITOR'S ACRONYM(S)

11. SPONSOR/MONITOR'S REPORT NUMBER(S)

12. DISTRIBUTION / AVAILABILITY STATEMENT
Approved for Public Release; Distribution Unlimited

13. SUPPLEMENTARY NOTES

14. ABSTRACT

We have demonstrated sympathetic tyrosine hydroxylase-positive (TH+) nerve fibers innervating breast tumors growing in the murine mammary fat pad. To study the role of the sympathetic nervous system in breast tumor progression, we used two approaches: 1) 6-hydroxydopamine (6-OHDA) to destroy sympathetic nerves and 2) desipramine to increase tumor NE concentration. 6-OHDA treatment reduced 4T1 tumor NE concentration by 60%, demonstrating that tumor NE is derived primarily from sympathetic nerve fibers. With sympathetic denervation, tumor weight and IL-6 concentration were reduced. Chronic desipramine treatment increased tumor NE, but it elicited only a small, transient increase in tumor growth. The relatively small magnitude of the treatment effects suggest that homeostatic mechanisms compensate for altered NE availability. Alternatively, the impact of sympathetic nerves may be spatially and/or temporally limited. Multiphoton laser scanning microscopy (MPLSM) provides the spatial and temporal resolution required to assess sympathetic nerve function in a growing tumor in vivo. Mice expressing enhanced green fluorescent protein gene fused to the TH promoter have been back-crossed to the BALB/c mouse strain to image TH+ nerves in 4T1 tumors using MPLSM. These experiments will more clearly define the impact of breast tumor sympathetic innervation with and without antiangiogenic treatment.

15. SUBJECT TERMS
breast cancer, sympathetic nervous system, angiogenesis, multiphoton laser scanning microscopy, VEGF, angiogenesis

16. SECURITY CLASSIFICATION OF:			**17. LIMITATION OF ABSTRACT**	**18. NUMBER OF PAGES**	**19a. NAME OF RESPONSIBLE PERSON**
a. REPORT	**b. ABSTRACT**	**c. THIS PAGE**			USAMRMC
U	U	U	UU	15	**19b. TELEPHONE NUMBER** *(include area code)*

Table of Contents

INTRODUCTION

Evidence from breast cancer patients and animal models of breast cancer suggests that stress can augment breast tumor growth and metastasis. Activation of the sympathetic nervous system (SNS) and release of norepinephrine (NE) from sympathetic nerve terminals is an important stress pathway. We have detected sympathetic noradrenergic nerve fibers in murine 4T1 mammary adenocarcinoma cells grown orthotopically in the mammary fat pad, but the functional interactions between sympathetic nerves and nearby target cells, including blood vessels, have not been investigated in breast cancer. We have demonstrated that catecholamine signaling can induce VEGF expression in some breast tumor cell lines *in vitro* [1]. Consequently, we believe that *SNS innervation is a key factor in encouraging angiogenesis, in preserving innervated tumor vessels from antiangiogenic therapy, and in providing a framework for rapid revascularization after effective therapy ceases.* We further believe that *therapeutic targeting of SNS signaling, using reagents already available in the clinic, is a promising method for inhibition of angiogenesis that will be synergistic with current antiangiogenic therapies and will greatly attenuate revascularization after effective therapy ceases.* Therefore, we propose to examine the impact of sympathetic innervation on angiogenesis and antiangiogenesis. We will test the following hypothesis: **Sympathetic innervation of breast tumors promotes angiogenesis and protects tumor blood vessels from antiangiogenic therapy.** Our first objective is to delineate the role of breast tumor sympathetic innervation and NE signaling in tumor growth, angiogenesis, and metastasis. A second objective is to explore the dynamic effect of catecholamine signaling on tumor vasculature using *in vivo* imaging with multiphoton laser scanning microcopy (MPLSM). The specific aims to achieve these objectives, broken down into individual tasks and progress made for each individual task, are described below. The time frame provided in parentheses after each task was taken from the statement of work.

BODY

Specific Aim 1. Determine how manipulation of sympathetic input influences breast cancer growth, angiogenesis, and metastasis.

Task 1. Initiate experiments to assess impact of sympathetic neurotransmitter removal/blockade in 4T1 tumors. (Months 1-6)

The first experiment had two objectives. First, to determine if reduced sympathetic input alters breast tumor growth and metastasis. Second, to determine if NE in orthotopic 4T1 tumors is derived primarily from sympathetic nerves or from the bloodstream. Chemical sympathectomy with the neurotoxin 6-hydroxydopamine (6-OHDA) ablates sympathetic noradrenergic nerve fibers and rapidly reduces NE concentration in innervated peripheral organs. 6-OHDA is taken up by the norepinephrine uptake mechanism present on sympathetic noradrenergic nerves. Inside the nerve terminal, 6-OHDA autooxidizes and destroys sympathetic noradrenergic nerves leading to a rapid depletion of NE in peripheral tissues. When administered to adult mice, 6-OHDA does not cross the blood-brain barrier. Because sympathetic nerve cell bodies in the spinal cord are not accessible to the neurotoxin, chemical sympathectomy with 6-OHDA is not permanent. When 6-OHDA treatment is discontinued, sympathetic nerves fibers can reenter the innervated tissue and restore innervation [2].

Methods.

Experimental Procedure. 6-OHDA was administered intraperitoneally (IP) 4 and 2 days prior to tumor implantation and thereafter every 5 days to prevent reinnervation and maintain a long-term sympathectomy [2]. The vehicle for 6-OHDA (0.01% ascorbate dissolved in saline) was injected IP into control animals in parallel with 6-OHDA treatment. Mice were injected with $2x10^5$ 4T1 tumor cells into a single mammary fat pad in mice under ketamine/xylazine anesthesia. Tumor growth (volume) was measured every 2-3 days using calipers. Tumor volume is calculated based on the equation: $V = 0.5 \times \text{length} \times \text{width}^2$. Personnel measuring the tumors were blinded to experimental group. In this experiment, mice were sacrificed 21 days after 4T1 tumor injection, and tumor, spleen and lungs were removed for further analysis.

4T1 tumor cells were grown in RPMI containing 10% fetal calf serum and penicillin and streptomycin. Cells were passaged when they reached 80% confluence. Cells were tested every month for mycoplasma contamination and new cells were obtained after 12 weeks in culture.

Norepinephrine, vascular endothelial growth factor (VEGF), IL-6, and pro-matrix metalloproteinase -9 (MMP-9) were measured by ELISA (R & D Systems, Minneapolis, MN) in tumor homogenates. Protein concentration in the tumor homogenates was determined by colorimetric BCA assay (Pierce Thermo Scientific, Rockford, IL).

Metastasis. Lungs were harvested and submerged in 4% paraformaldehyde for 72 h, followed by 30% sucrose for 24 h. The lungs were cut on a cryostat into 30 µM-thick sections every 100 µM for hematoxylin and eosin (H&E) staining. Metastatic foci, visualized using a 4X objective lens by standard light microscopy, were counted in each tissue section.

Results. The extent of sympathetic denervation after chronic 6-OHDA treatment (for 25 days post the initial 6-OHDA injection) was determined by comparing NE concentration in the orthotopic tumor to NE concentration in the spleen, an organ highly susceptible to 6-OHDA-induced denervation. In the tumor, NE concentration (NE per tumor wet weight or NE per µg protein) and total tumor NE was reduced 40-60% in 6-OHDA–treated mice compared to vehicle controls (Fig. 1 A-C). By comparison, NE concentration was much higher in the vehicle control spleens, and NE was reduced 75-80% in 6-OHDA-treated mice (Fig. 1D-F). In 6-OHDA-treated mice, tumor weight was reduced 27%, but this decrease did not reach statistical significance (Fig. 2A; two-tailed t-test, p = 0.19). A 21% reduction in spleen weight in sympathectomized mice was statistically significant (Fig. 2B, two-tailed t-test, p = 0.014). Body weight was not different between vehicle and 6-OHDA-treated mice at the time of sacrifice (data not shown). No change in tumor volume was detected at any time point (Fig. 2C). The concentration of tumor IL-6 was reduced approximately 30% (Fig. 2E; two-tailed t-test, p=0.07), but VEGF (Fig. 2D) and pro-MMP-9 (Fig. 2F) concentrations were unchanged (two-tailed t-test, p=0.8, 0.35 respectively).

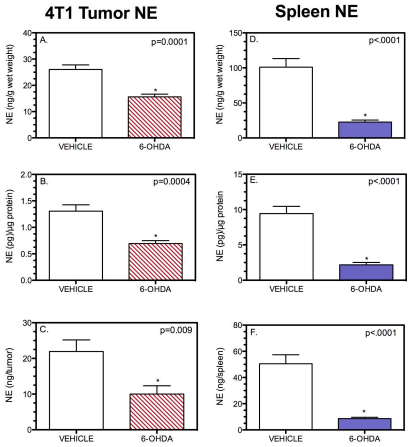

Fig. 1. NE concentration is reduced in chemically sympathectomized mice. NE concentration and total NE measured in 4T1 tumors grown in the mammary fat pad and in the spleen of mice treated with vehicle (n=10) or 6-OHDA (n=9), 21 days after 4T1 injection. Results shown are mean ±SEM. Asterisk indicates significance by student's t-test (p<0.05) vs vehicle control.

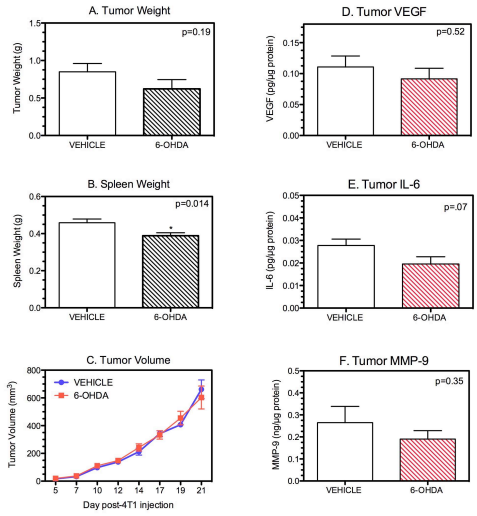

Fig. 2. Tumor growth and cytokine content in chemically sympathectomized mice. Tumor weight and cytokine content were measured 21 days after 4T1 injection in the same animals shown in Fig. 1. Results shown are mean ±SEM. Asterisk indicates significance by student's t-test (p<0.05) vs vehicle control.

By H&E staining, tumor metastases were observed in the lung as foci of tightly packed cells with dark blue staining (high nuclear to cytoplasmic ratio). Examples of the metastatic foci that were counted in each tissue section are shown in Fig. 3A-C. The paraformaldehyde-fixed 30 µM-thick sections exhibited darker than expected background when stained by H&E, but we were able to distinguish and count metastasis. No significant changes in the number of tumor metastases were detected in the 6-OHDA-treated mice compared to vehicle controls (Fig. 3D).

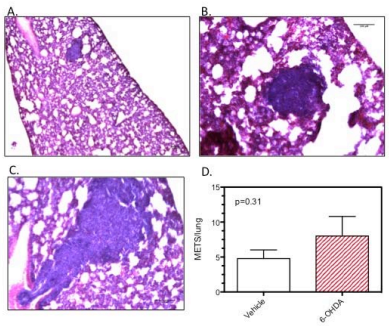

Fig. 3. (A-C) Examples of metastatic foci in lungs. (D) Quantification of metastatic foci. Lungs were from same animals shown in Figs 1 and 2. No statistical difference in lung metastases was detected.

Discussion/Conclusions. Although NE concentration in orthotopic 4T1 tumors was low compared to the spleen, 6-OHDA treatment reduced tumor NE concentration significantly. This experiment demonstrates the majority of NE present within orthotopic mammary tumors is derived from sympathetic noradrenergic nerve fibers. The inability of 6-OHDA to deplete NE in the tumor as well as the spleen may be because the remaining NE is derived from the blood and is not susceptible to sympathetic nerve ablation. Another possibility is that 6-OHDA not able to penetrate the tumor parenchyma due to the leaky tumor vasculature [3].

The functional impact of loss of sympathetic nerves and depletion of norepinephrine was reduced tumor weight and reduced tumor IL-6 concentration. This result suggests that the sympathetic nervous system potentiates tumor weight and IL-6 production, but the magnitude of these effects was small and did not reach statistical significance. 4T1 elicits a large hematogenous response, as indicated by enlarged spleens in 4T1-bearing mice. (Normal mouse spleen weight is ~ 100 mg, compared to ~ 400 mg in the tumor-bearing mice at three weeks post-tumor injection.) The reduction in spleen and tumor weight in sympathectomized mice suggests that the sympathetic nervous system facilitates the hematogenous response to 4T1, and raises the possibility that the reduced IL-6 is due to reduced migration of an IL-6-producing cell type, such as macrophages, into the tumor. Alternatively, the reduction in IL-6 concentration may be due to decreased production of IL-6 within the tumor itself.

The relatively small impact of sympathetic denervation on our measures of tumor pathogenesis may be due to incomplete denervation. Alternatively, the relatively small magnitude may be a function of the long-term sympathetic ablation. Because our goal was to test the impact of sympathetic denervation throughout the growth and progression of the tumor, the treatment regimen was designed to induce a long-lasting sympathectomy. Chronic loss of sympathetic tone and reduced norepinephrine may elicit homeostatic mechanisms to counter-balance the loss of catecholamines in innervated tissues, and thus minimize the effects of depletion of norepinephrine. One example of such a homeostatic mechanism following 6-OHDA treatment is increased catecholamine synthesis by the adrenal medulla [4]. We believe that concurrent adrenergic receptor blockade may be necessary to reveal the full impact of loss of sympathetic nerve fibers. To test this possibility, we will treat denervated mice with a ß-adrenergic receptor (ß-AR) antagonist after 6-OHDA treatment has been initiated to prevent the interaction of the NE or epinephrine (EPI) with ß-adrenergic receptors after sympathectomy. We predict this treatment will reduce the impact of a homeostatic elevation of either NE or EPI following sympathectomy, and lead to more robust effects of sympathetic ablation.

Task 2. Initiate experiments to assess impact of elevation of NE in 4T1 tumors (NE and Desipramine) (Months 7-12)

We have also examined the impact of elevated sympathetic signaling on 4T1 tumor growth, angiogenesis, and metastasis by increasing NE availability. To achieve a prolonged elevation of NE, mice were implanted with 21-day slow-release pellets containing desipramine (DMI) (Innovative Research of America, Sarasota, FL). DMI is a tricyclic antidepressant that prevents NE uptake, thereby increasing NE availability [5].

Methods.

Experimental Procedure. In DMI Experiment 1, mice were implanted subcutaneously with pellets containing either 1.5 mg or 5 mg DMI or placebo 2 days prior to 4T1 tumor injection. Mice were injected with $2x10^5$ 4T1 tumor cells into a single mammary fat pad. Tumor volume was determined every 2-3 days as described above. VEGF, IL-6, pro-MMP-9 and NE were measured by ELISA as described above.

Metastasis. Lungs were harvested and submerged in formalin prior to paraffin embedding. The lobes of both lungs were sectioned into 4-µM-thick sections every 100 µM for hematoxylin and eosin (H&E) staining. Metastatic foci, visualized using a 4X objective lens by standard light microscopy, were counted in each tissue section.

Results. When tumor growth was analyzed up through day 16 post–4T1 injection by two-way repeated measures ANOVA, a significant interaction of time by treatment was detected (p=0.03) with a trend towards a main effect (p=0.1) (Fig 4A). By Bonferonni's post-hoc analysis, the 5 mg DMI group was greater than placebo at days 14 and 16. When tumor volumes at day 19 and day 21 were included in the analysis, the main effect and interaction were eliminated (interaction, p = 0.4; main effect, p = 0.8) (Fig. 4B). At the time of sacrifice, day 21 after 4T1 injection, there were no differences in tumor weight (Fig. 4C). Tumor VEGF and IL-6 concentration did not differ between the three groups (Fig. 5A, B). However, total pro-MMP-9 concentration was significantly elevated in the mice that received the 5 mg DMI pellet compared to the placebo and the 1.5 mg DMI group (Fig. 5C). Tumor NE was not elevated in any group at the time of sacrifice (Fig. 5D), but in this experiment, animals were sacrificed two days after the 21-day pellets were no longer releasing DMI into the bloodstream. This experiment demonstrated that 5 mg DMI transiently increased tumor growth, but the effect was no longer present by day 21, a time when tumor growth had entered an exponential growth phase (Fig. 4B).

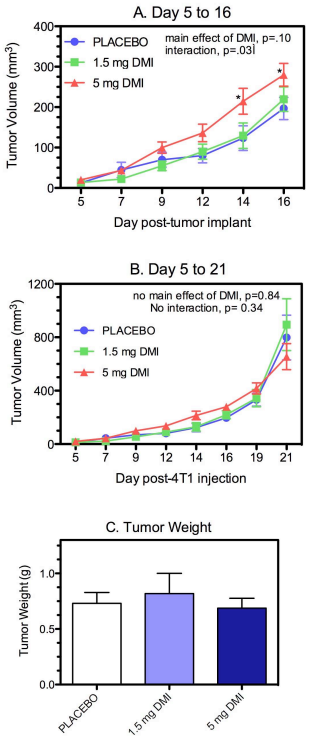

Fig. 4. DMI treatment transiently increased tumor growth. In this experiment mice were implanted subcutaneously with 21-day release pellets 2 day prior to 4T1 injection. Results are expressed as mean±SEM of n=6-7 mice per group. Tumor weight was determined 21 days after 4T1 implantation. Description of statistical analysis can be found in the text.

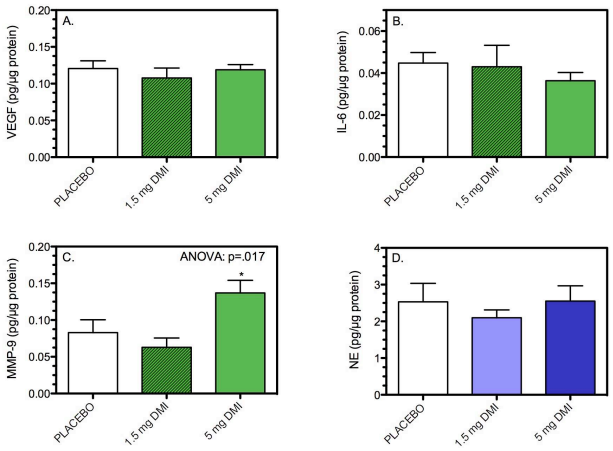

Fig. 5. NE and cytokine analysis in DMI-treated mice described in Fig. 4. Data were analyzed by one-way ANOVA. Asterisk indicates statistical signficance versus other two groups by Neuman-Keuls post-hoc analysis ($p<0.05$).

In this experiment, the H&E stained 4 µM-thick sections from paraffin-embedded tissue showed more appropriate lighter cytoplasmic staining (Fig. 6A-C). No differences in metastases were detected between the three treatment groups.

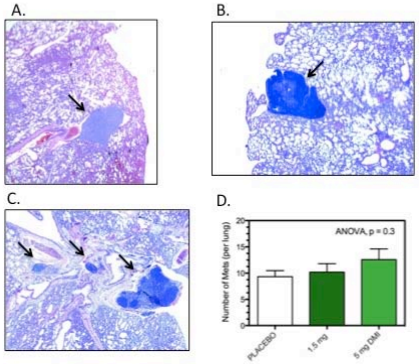

Fig. 6. Examples of lung metastis with DMI treatment (A-C). Arrows indicate metastatic foci. Quantification of metastases shown in D. The treatment of these mice is described in Fig. 4.

In the next experiment (DMI Experiment 2), a similar experimental procedure was followed, except only the 5 mg DMI dosage was tested. In this experiment, mice were sacrificed at day 19 post-4T1 injection, when the 21-day pellets would still release DMI into the blood stream.

Results. At day 19 post-4T1 injection, tumor NE concentration was significantly elevated (Fig. 7A). However, no difference in tumor growth was detected over time (Fig. 7B), and tumor weight (Fig. 7C), tumor VEGF (Fig. 7D), IL-6 (Fig. 7E), and pro-MMP-9 (Fig.7F) were unaltered by DMI treatment. Furthermore, no significant alterations in lung metastasis were noted (Fig. 7G). We noted, however, that the rate of tumor growth was greater in this experiment compared with the previous experiment. The next experiment was designed to determine if tumor growth rate is a factor determining the response to elevated NE.

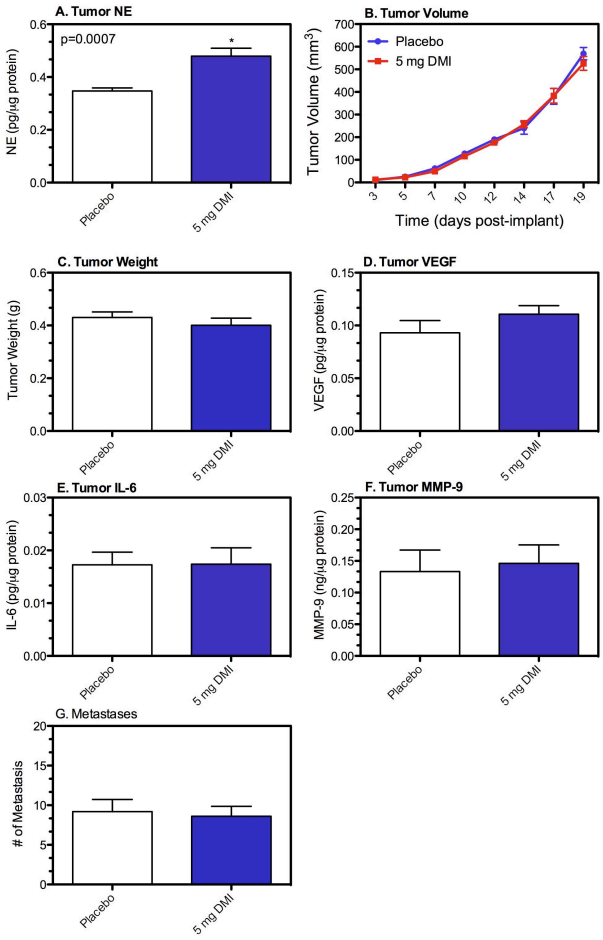

Fig. 7. DMI Experiment (2). In this experiment, mice were implanted with 5 mg DMI or placebo pellets two days before 4T1 injection. Mice were sacrificed day 19 post-4T1 injection. Results shown are mean ± SEM of 9-10 mice per group. Results were analyzed by student's t-test. Asterisk indicates significance ($p<0.05$).

In DMI Experiment 3, a 2-fold lower concentration of 4T1 tumor cells ($1x10^5$ cells) was injected into the mammary fat pad to reduce the rate of tumor growth. As in the previous experiments, pellets containing either 5 mg DMI or placebo were subcutaneously implanted two days prior to tumor cell injection. All other experimental procedures were as described above.

Results. 4T1 tumor volume was elevated in the mice implanted with DMI pellets days 12-14 post 4T1 injection, but the effect was transient. When tumor volume was analyzed through day 14, there was a significant main effect of treatment ($p = 0.02$) by two-way repeated measures ANOVA. By Bonferonni's post-hoc analysis, tumor volume was greater in the DMI group at day 12 and day 14 (Fig. 8A). However, when day 17 and day 19 were included in the analysis, there was no main effect of treatment, $p = 0.24$ or treatment by time interaction $p=0.6$ (Fig. 8B). Tumor weight at sacrifice (day 19) was slightly, but not significantly elevated (Fig. 8C; two tailed student's t-test, $p=0.12$). Furthermore, although there was a significant elevation in tumor NE concentration (Fig. 9A), tumor concentrations of VEGF (Fig. 9B), IL-6 (Fig. 9C), and pro-MMP-9 (Fig. 9D) were not altered in the DMI treated mice. Interestingly, the number of lung metastases was significantly reduced in the DMI-treated mice (Fig. 9E).

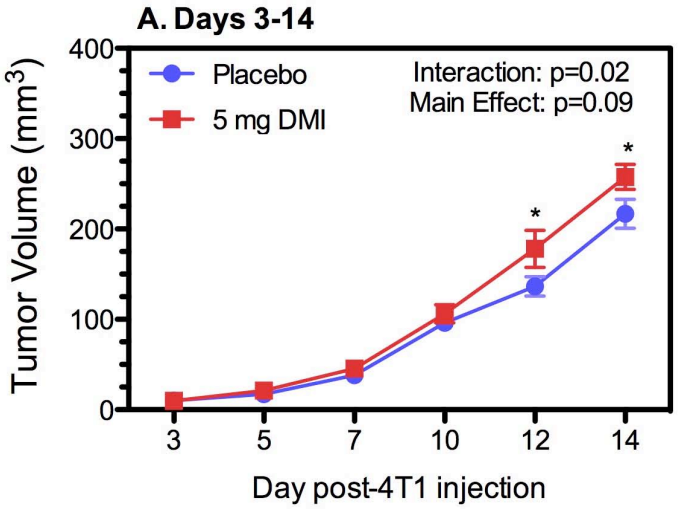

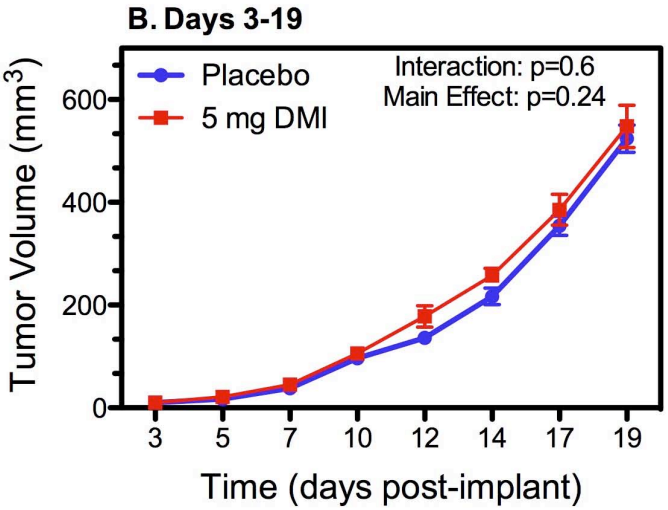

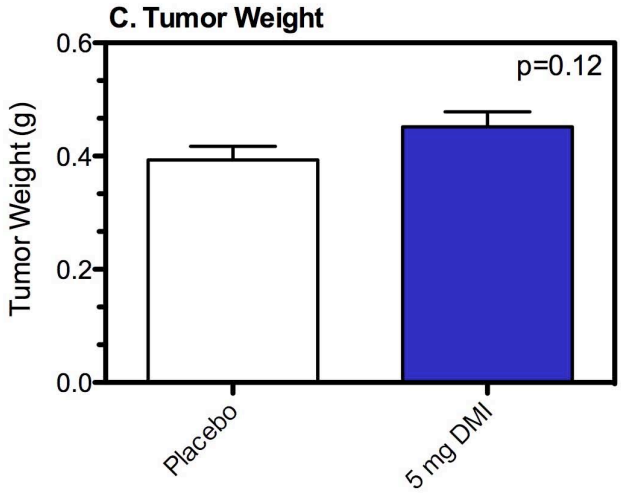

Fig. 8. DMI Experiment 3. 2-fold lower 4T1 cells were injected into the mammary fat pad 2 days after implantation with 5 mg DMI or placebo pellets. Results shown are mean ± SEM, n=9-10 mice per group. Statistical analysis is described in the text.

Discussion/Conclusions. From the

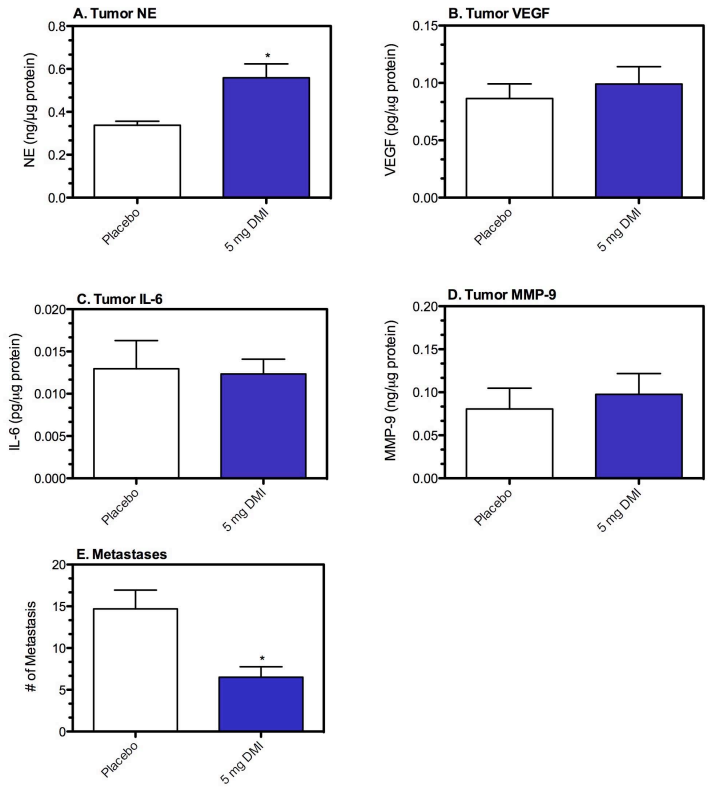

Fig. 9. DMI Experiment 3. NE and cytokines were measured in orthotopic 4T1 tumors. These are the same mice as shown in Fig. 8. Statistical analysis by student's t-test. Asterisks indicate significance vs placebo ($p<0.05$).

DMI experiments, we learned that 4T1 tumor NE concentration was elevated by 5 mg DMI. However, this increase in NE elicited only transient increases in tumor volume not robust enough to overcome differences in tumor growth between experimental repetitions. The analysis of tumor concentrations of VEGF, IL-6, pro-MMP-9, and lung metastasis showed only occasional significant alterations. In the experiment in which lower 4T1 cell numbers were reduced, the number of lung metastasis was unexpectedly reduced, in association with a slight elevation in tumor weight. In the absence of changes in tumor pro-metastatic cytokines such as IL-6 and MMP-9, it is possible that the reduced metastasis in this experiment was related to alterations in NE concentration in the lung. In experiments currently underway, we are testing a higher DMI concentration and varying the number of 4T1 tumor cells injected. We will also test the effects of NE directly administered in pellet form as proposed.

Based on recent reports (including our own data), we have been surprised to see few changes in tumor cytokines despite changes in NE levels. VEGF production in several ß-AR-expressing cell lines is altered by ß-AR stimulation and by stressor exposure, including the breast cancer cell lines MB-231 and MB-231BR [1]. By radioligand binding, we have discovered that 4T1 express no detectable ß-AR, and direct 4T1 ß-AR stimulation *in vitro* does not alter 4T1 VEGF production (Fig. 10A, B). 4T1 tumors do not produce detectable levels of MMP-9 and IL-6 under our *in vitro* culture conditions. Therefore, ß-AR-expressing stromal cell populations, including endothelial cells, fibroblasts, and cells of the immune system, must be considered the primary targets for sympathetic innervation in breast tumors that do not express ß-AR. These findings do not change the objectives or focus of this proposal, but it does change our prediction as to the nature of the primary target cells of sympathetic innervation within a breast tumor. In tumors in which ß-AR expression and signaling is low or undetectable, ß-AR-expressing tumor stromal cells may be the key targets of sympathetic innervation with less direct input via ß-AR stimulation of the cancer cells themselves.

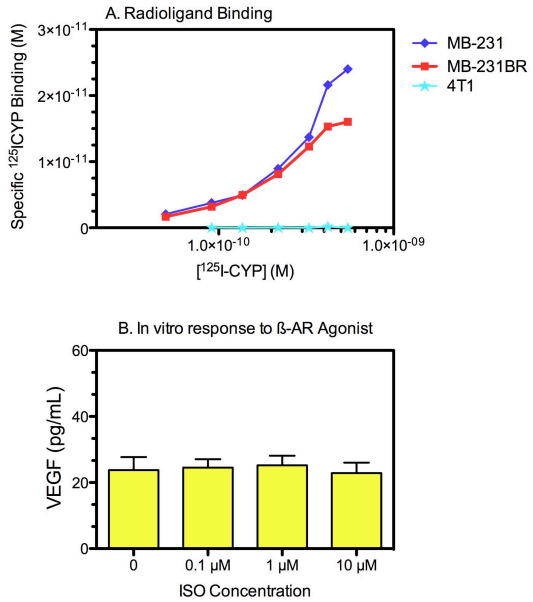

Fig. 10. 4T1 cells express no detectable ß-AR protein and do not respond to ß-AR stimulation in vitro. (A) Radioligand binding assay using the ß-antagonist cyanopindolol shows high levels of ß-AR by two human breast cancer cell lines MB-231 and MB-231BR. 4T1 displays no detectable specific ICYP binding. Results are representative of 3 experimental repetitions (B) Stimulation of 4T1 cells with the ß-agonist isoproterenol (ISO) does not alter VEGF production by 4T1 in vitro. Results are representative of 2 experimental repetitions.

Another possible explanation for our results is the relatively limited distribution of tumor sympathetic nerves. Sympathetic innervation appears primarily restricted to the periphery of the tumor, and may limit the impact of sympathetic nerves to regions immediately surrounding the nerves. In addition, the relatively rapid growth of 4T1 may limit the impact of sympathetic nerves on tumor pathogenesis to a particular time in the growth of the tumor. I*n vivo* imaging with MPLSM, proposed in Specific Aim 4, is particularly well-suited to provide the spatial and temporal resolution required to assess sympathetic nerve function in a growing tumor. We have begun to explore the use of MPLSM to examine the interactions between sympathetic nerves and tumor blood vessels -- see Specific Aim 4 for progress in this area.

Specific Aim 2. Determine the plasticity of sympathetic innervation following removal of blood vessels by antiangiogenic therapy and revascularization following termination of antiangiogenic therapy.

Task 3 (Months 11-15). No progress to report. Experiments testing antiangiogenic therapy as described in specific Aim 2 and 3 will begin in April, 2011.

Specific Aim 3. Determine the impact of removal of sympathetic input on the effectiveness of antiangiogenic therapy in breast tumors.

Task 4. Initiate experiments to assess impact of increased NE and sympathetic blockade with antiangiogenic therapy. (Months 15-20). No progress to report.

Specific Aim 4. Dynamically characterize the relationship between breast tumor blood vessels and sympathetic innervation *in vivo* using MPLSM.

Task 5. Back-cross TH-EGFP transgene to BALB/cByJ background (Months 1-18).
Task 5a. Breed TH-EGFP mice to BALB/cByJ mice for 10 generations
We have proposed to examine sympathetic nerve interactions with blood vessels in breast tumors *in vivo* using MPLSM. MPLSM allows *in vivo* 3D imaging in tumors with sub micron resolution to a depth of ~0.5 mm. We have employed a transgenic mouse line in which the enhanced green fluorescent protein (EGFP) reporter gene has been inserted immediately upstream of the coding sequence for tyrosine hydroxylase (TH) (STOCK Tg(Th-EGFP)DJ76Gsat/Mmnc, purchased from Mutant Mouse Regional Resource Center). This strain was developed originally by Nathaniel Heintz, Ph.D., The Rockefeller University, as part of the GENSAT Project. TH is the rate-limiting enzyme in the norepinephrine/epinephrine biosynthetic pathway, and is used as a marker for sympathetic

noradrenergic nerve fibers. We will use this feature to observe the relationship between sympathetic nerves and tumor blood vessels with MPLSM.

To detect EGFP-TH+ nerves in 4T1 tumors, we have back-crossed the original TH-EGFP transgenic line on the Swiss-Webster background to the BALB/c strain for 4 generations. (The fifth generation pups were born in March.) Using speed congenic analysis services provided by Taconics Laboratory, we have been able to achieve 98% BALB/c background in 4 generations. We have grown 4T1 tumors in the mammary fat pad of TH-EGFP.BALB females and subcutaneously in TH-EGFP.BALB males from the F2 and F3 generations. We have begun to characterize TH-EGFP expression in 4T1 tumors and other peripheral tissues *ex vivo* by TPLSM. For *ex vivo* imaging of these tissues, harvested tissues were sliced into sections approximately 5 mm thick. EGFP was excited at 930 nm and fluorescent emission (535/40 nm) was detected with a photomultiplier tube. Laser power exiting the objective lens was approximately 80 mW.

EGFP+ nerve fibers were observed in spleen (Fig. 11A, B, arrows), but a cell-associated fluorescence was also detected that was clearly not nerve fibers. This autofluorescence was also detected in spleen of wild-type mice (data not shown). In the 4T1 tumors, nerve fibers were detected coursing through the periphery of the tumor (Fig. 11C-F), as expected from the immunohistochemical staining for TH. In addition, single fibers were also detected as far as ~250 μM into the tumor in some mice (Fig. 11D, red arrows). In the tumors, the cell-associated autofluorescence was also detected. Our goals are to minimize the autofluorescence by testing varying excitation wavelengths and reducing laser power. Once optimal imaging conditions are established, we will begin to assess TH-EGFP+ nerve interactions with blood vessels in a growing tumor and with antiangiogenic therapy.

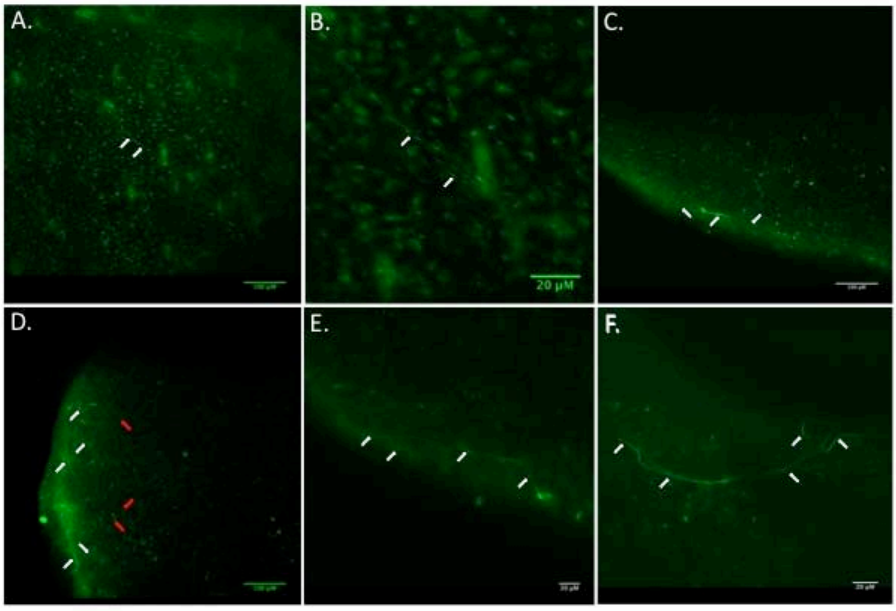

Fig. 11. MPLSM detection of TH-EGFP nerve fibers and autofluorescent cells in spleen (A,B) and orthotopic 4T1 tumor grown in a TH-EGFP.BALB/c female mouse. Imaging parameters are described in the text.

Task 6. Image 4T1 blood vessels and sympathetic nerves in EGFP-TH transgenic mice with antiangiogenic therapy and cessation of therapy using MPLSM. (Months 18-24).

The transgenic mice EGFP.BALB/c bred at the University of Rochester in Task 5 will be used here.
No progress to report.

KEY RESEARCH ACCOMPLISHMENTS

- Determined that most NE present in orthotopic mammary tumors is derived from sympathetic nerve terminals.
- Characterized tumor growth and metastasis in response to sympathetic ablation with 6-OHDA and to increased NE by uptake blockade with DMI.
- Characterized 4T1 ß-adrenergic receptor expression, signaling and function in vitro.
- TH-EGFP transgene back-crossed to BALB/c mouse strain (THEGFP.BALB/c).
- By MPLSM, confirmed the presence of TH-EGFP in *ex vivo* 4T1 breast tumors grown in TH-EGFP.BALB/c mice.

REPORTABLE OUTCOMES

Poster Presentations:

EVIDENCE FOR SYMPATHETIC NERVOUS SYSTEM AND NOREPINEPHRINE REGULATION OF BREAST CANCER PATHOGENESIS. MJ Szpunar, KS Madden, KM Liverpool, EB Brown. 15th Annual University of Rochester Cancer Center Symposium. Rochester, NY (November 11, 2010.)

SYMPATHETIC NERVOUS SYSTEM INNERVATION AND FUNCTION IN A BETA-ADRENERGIC RECEPTOR NEGATIVE BREAST CANCER MODEL IN MOUSE
Mercedes J. Szpunar; Kelley S. Madden, PhD; Khawarl M. Liverpool; and Edward B. Brown, PhD. Psychoneuroimmunology Research Society Annual Meeting, PNI Mechanisms of Disease: From Pathophysiology to Prevention and Treatment, June 8-11, 2011; Chicago, IL.

DETECTION OF SYMPATHETIC TYROSINE HYDROXYLASE-POSITIVE (TH+) NERVE FIBERS IN ORTHOTOPIC MAMMARY TUMORS BY MULTIPHOTON LASER SCANNING MICROSCOPY (MPLSM). Kelley S. Madden, Mercedes J. Szpunar, Echoe M. Bouta, Edward B. Brown. Psychoneuroimmunology Research Society Annual Meeting, PNI Mechanisms of Disease: From Pathophysiology to Prevention and Treatment, June 8-11, 2011; Chicago, IL.

Publications

Madden, K.S., M.J. Szpunar, E. B. Brown. 2011. ß-Adrenergic Receptors (ß-AR) regulate VEGF and IL-6 production by divergent pathways in high ß-AR-expressing breast cancer cell lines. Breast Cancer Res. Treat. *Published online Jan 13, 2011*. DOI: 10.1007/s10549-011-1348-y

Animal Model:

TH-EGFP transgene back-crossed to BALB/c background.

CONCLUSIONS

We have shown that sympathetic noradrenergic nerve fibers are the primary source of NE in orthotopic breast tumors. This implies that manipulation of sympathetic nerve fibers (ablation) or NE release (DMI) should impact tumor growth. Yet, sympathectomy-induced ablation of NA nerve fibers and reduction in NE elicited only a small change in tumor weight. Small or no changes in VEGF, IL-6 or pro-MMP-9 or metastasis to the lung were detected. Similarly, increased NE in 4T1 tumors elicited only small, transient increases in primary tumor growth and little or no change in VEGF, IL-6, pro-MMP-9, or metastases to the lung. We envisioned an interaction between sympathetic nerves and angiogenesis via the tumor cells and elevated tumor cell production of VEGF. Our finding that 4T1 expresses no detectable ß-AR and is incapable of signaling through these receptors suggests that in this breast tumor model, neural interactions with stromal cells, especially the endothelial cells, may be most relevant. It should be pointed out that there is very limited knowledge of primary breast tumor cell ß-AR expression. We have screened a number of human breast cancer cell lines for ß-AR expression and found that most of them (with the notable exceptions of MB-231 and MB-231BR) express low to no ß-AR protein. If these results reflect primary breast tumor cell ß-AR expression, the ß-AR-expressing tumor stromal cells within a primary tumor may be the targets of sympathetic innervation, and their interactions with the noradrenergic nerve fibers need to be understood, as we have proposed in this grant.

Another possible explanation for our results is the restricted anatomical distribution of tumor sympathetic nerves to the periphery of the tumor. This may limit the impact of the sympathetic nerves to the areas surrounding the nerves.

Combined with the relatively rapid growth of 4T1, the impact of sympathetic nerves on tumor pathogenesis may be limited to a particular anatomical site and time in the growth of the tumor. We saw hints that the effects of elevated DMI are transient and are no longer present either when the tumor reaches a certain size or are in an exponential phase of growth. I*n vivo* imaging with MPLSM proposed in Specific Aim 4 is particularly well-suited to provide the spatial and temporal resolution required to assess sympathetic nerve function in a growing tumor.

A third possibility for our negative results is the homeostatic mechanisms that are initiated after perturbation of the sympathetic nervous system. We have discussed potential mechanisms in the results section above and the experiments to test this possibility. The drive towards homeostasis is critical in all biological systems, and must be understood, especially in the context of cancer, where normal check points in cellular growth and differentiation are impaired. It is clear that a growing tumor can co-opt host cells to ensure continued tumor survival and growth – initiation of angiogenesis being just one example. Our results suggest that, at least in this breast cancer model, homeostasis of the sympathetic nervous system is intact – and the host can accommodate loss of the sympathetic nerves and an increase in NE release and availability. Therefore, we will determine if experimental manipulations to block this homeostasis can lead to more marked changes in tumor growth and metastasis.

Our goal is to define the role of the sympathetic nervous system in the 4T1 breast tumor model. Our results thus far have begun to alter our view of the nature of the primary target cells of sympathetic innervation within a breast tumor. Therefore, the impact of a stressor that elicits NE or EPI release may vary depending on the ß-AR expression patterns within breast tumors. This is a key point that needs further investigation. Our goal ultimately is to apply our findings to treatment of human breast cancer and metastasis, but before therapies such as ß-AR blockade, can be proposed, a more sophisticated understanding of the impact of sympathetic nervous system activation and release of NE is required. Understanding the impact of sympathetic innervation on relevant target cells within molecularly heterogeneous breast tumor models is required before attempting therapies that focus on manipulation of the sympathetic nervous system.

REFERENCES

1. Madden KS, Szpunar MJ, Brown EB (2011) beta-Adrenergic receptors (beta-AR) regulate VEGF and IL-6 production by divergent pathways in high beta-AR-expressing breast cancer cell lines. Breast Cancer Res Treat. doi:10.1007/s10549-011-1348-y

2. Lorton D, Hewitt D, Bellinger DL, Felten SY, Felten DL (1990) Noradrenergic reinnervation of the rat spleen following chemical sympathectomy with 6-hydroxydopamine: Pattern and time course of reinnervation. Brain, Behavior, and Immunity 4:198-222

3. Jain RK (2001) Normalizing tumor vasculature with anti-angiogenic therapy: a new paradigm for combination therapy. Nat Med 7 (9):987-989

4. Mueller RA, Thoenen H, Axelrod J (1969) Adrenal tyrosine hydroxylase - Compensatory increase in activity after chemical sympathectomy. Science 163:468-469

5. Zhao Z, Baros AM, Zhang HT, Lapiz MD, Bondi CO, Morilak DA, O'Donnell JM (2008) Norepinephrine transporter regulation mediates the long-term behavioral effects of the antidepressant desipramine. Neuropsychopharmacology 33 (13):3190-3200

APPENDICES: Attach all appendices that contain information that supplements, clarifies or supports the text. Examples include original copies of journal articles, reprints of manuscripts and abstracts, a curriculum vitae, patent applications, study questionnaires, and surveys, etc.

None